

Infinesimal Perturbation Analysis of Stochastic Flow Models with Delays: Application to Multi-Intersection Traffic Light Control ^{*}

Rui Chen and Christos G. Cassandras
 Division of Systems Engineering
 Boston University, Boston, MA 02215, USA
 E-mail:{ruic, cgc}@bu.edu

Abstract—We extend Stochastic Flow Models (SFM), which are used for a large class of hybrid systems, by including the delays which typically arise in flow movement. We apply this framework to the multi-intersection traffic light control problem by including transit delays for vehicles moving from one intersection to the next. Using Infinitesimal Perturbation Analysis (IPA) for this SFM with delays, we derive new on-line gradient estimates of several congestion cost metrics with respect to the controllable green and red cycle lengths. The IPA estimators are used to iteratively adjust light cycle lengths to improve performance and, in conjunction with a standard gradient-based algorithm, to obtain optimal values which adapt to changing traffic conditions. We introduce two new cost metrics to better capture congestion and show that the inclusion of delays in our analysis leads to improved performance relative to models that ignore delays.

I. INTRODUCTION

Stochastic Flow Models (SFM) capture the dynamic behavior of a large class of hybrid systems [1],[2]. The basic building block in a SFM is a queue (buffer) whose fluid content is dependent on incoming and outgoing flows which may be controllable. By connecting such building blocks together, one can generate stochastic flow networks which are encountered in application areas such as manufacturing systems [3], chemical processes [4], water resources [5], communication networks [6] and transportation systems [7]. Figure 1 shows a two-node SFM, in which an on-off switch controls the outgoing flow for each node. When the switch at the output of node 1 is turned on, a “flow burst” is generated to join the downstream node 2. It is commonly assumed that this flow burst can instantaneously join the downstream queue, thus ignoring potentially significant delays before this can happen. As an example, if the two nodes in Fig. 1 represent neighboring intersections in a traffic system, bursts of vehicles are generated whenever the light turns green at node 1. However, depending on the distance between intersections, there is a finite delay involved in the vehicle burst joining the downstream queue. Ignoring such delays impacts the behavior of the system and any control mechanism developed to achieve a desirable performance.

Control mechanisms used in SFMs often involve gradient-based methods in which the controller uses estimates of the performance metric sensitivities with respect to controllable parameters in order to adjust the values of these parameters and improve (ideally, optimize) performance. Infinitesimal Perturbation Analysis (IPA) is a method of general applicability to stochastic hybrid systems [2],[8] through which gradients of performance measures may be estimated with

respect to several controllable parameters based on directly observable data. There are several advantages associated with the use of IPA: (i) IPA estimates have been shown to be unbiased under very mild conditions [2]. (ii) IPA estimators are robust with respect to the stochastic processes used in our model. (iii) IPA is event-driven, hence scalable in the number of events in the system, not the space dimensionality. (iv) IPA possesses a decomposability property [9], i.e., IPA state derivatives become memoryless after certain events take place. (v) The IPA methodology can be easily implemented on line, allowing us to take advantage of directly observed data. While IPA has been extensively used in SFMs, the effect of delays between adjacent nodes, as described above, has not been studied to date. The contribution of this paper is to incorporate delays in the flow bursts that are created by on-off switching control (see Fig. 1) into the standard SFM and to develop the necessary extensions to IPA for such systems. The key motivation for this work is the Traffic Light Control (TLC) problem in transportation networks, which consists of adjusting green and red signal settings in order to control the traffic flow through an intersection and, more generally, through a set of intersections and traffic lights in an urban roadway network. The ultimate objective is to minimize congestion in an area consisting of multiple intersections. Many methods have been proposed to solve the TLC problem, including expert systems, genetic algorithms, reinforcement learning and several optimization techniques; a more detailed review of such methods may be found in [10]. Perturbation analysis methods were used in [11],[12]. IPA was used in [13] and [14] for a single intersection and extended to multiple intersections in [7] and to quasi-dynamic control schemes in [10]. However, all this work to date has assumed that vehicles moving from one intersection to the next experience no delay. In this paper, this assumption is relaxed and we derive IPA gradient estimators and adaptive controllers which adjust red-green cycles (treated as controllable parameters) on line taking delays into account in order to optimize selected performance metrics (cost functions). We study several such cost functions in an effort to better capture “congestion” in traffic systems: (i) The mean of the total weighted queue lengths at two adjacent intersections, as in prior work, (ii) The mean of the total weighted powers of queue lengths, thus placing higher costs on longer vehicle backlogs, and (iii) The fraction of time that queue lengths are larger than given thresholds, an alternative way of placing higher costs on longer vehicle backlogs. The rest of the paper is organized as follows. In Section II, we extend the standard multi-node SFM to include delays and in Section III we adapt this model to the TLC problem and introduce two new cost metrics for congestion.

^{*} Supported in part by NSF under grants ECCS-1509084 and IIP-1430145, by AFOSR under grant FA9550-15-1-0471, and by the MathWorks.

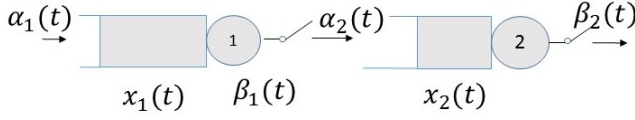


Fig. 1. A two-node SFM.

In Section IV, we carry out IPA. In Section V, we provide simulation examples comparing performance results between a model considering traffic delays and one which does not, showing that the former achieves improved performance.

II. STOCHASTIC FLOW MODELS WITH DELAYS

Consider a two-node SFM as in Fig. 1 and let $\{\alpha_i(t)\}$ and $\{\beta_i(t)\}$, $i = 1, 2$, be the *incoming flow processes* and *outgoing flow processes* respectively. We define a state vector $x(t) = [x_1(t), x_2(t)]$, where $x_i(t) \in \mathbb{R}^+$ is the flow content of queue i (we assume that all variables are left-continuous.) The dynamics of this SFM are given by

$$\dot{x}_i(t) = \begin{cases} 0 & \text{if } x_i(t) = 0, \alpha_i(t) \leq \beta_i(t) \\ & \text{or } x_i(t) = c_i, \alpha_i(t) \geq \beta_i(t) \\ \alpha_i(t) - \beta_i(t) & \text{otherwise} \end{cases} \quad (1)$$

where c_i is the capacity of queue i (which we will assume to be infinite in the rest of this paper). In addition, the presence of the switching controller $u_i(t) \in \{0, 1\}$, $i = 1, 2$, implies that $\beta_i(t)$ depends on the on-off state of node i , therefore

$$\beta_i(t) = \begin{cases} h_i(t) & \text{if } u_i(t) = 1 \\ 0 & \text{otherwise} \end{cases}$$

where $h_i(t)$ is the instantaneous outgoing flow rate at node i . Thus, when $u_1(t) = 1$, $t \in [t_1, t_2]$, $u_1(t_1^-) = 0$, a flow burst is created at node 1 (assuming that $x_1(t_1) > 0$). In general, several such flow bursts may be created over $(t_1, t_2]$, depending on values of $\alpha_1(t)$, $h_1(t)$, $t \in (t_1, t_2]$. If for example, $\alpha_1(\tau_1) = 0$ for some $\tau_1 \in (t_1, t_2)$, this marks the end of the first burst; if $\alpha_1(\tau_2) > 0$ for some $\tau_2 > \tau_1$, $\tau_2 \in (\tau_1, t_2)$, then a second flow burst is initiated at time τ_2 . In a typical SFM, we ignore the delay incurred by any such flow burst being transferred between nodes and assume that it instantaneously joins the queue at node 2. Under this assumption,

$$\alpha_2(t) = \begin{cases} \alpha_1(t) & \text{if } x_1(t) = 0, \alpha_1(t) \leq \beta_1(t) \\ \beta_1(t) & \text{otherwise} \end{cases}$$

In what follows, we enhance the SFM to include the aforementioned delay and provide the conditions under which a flow burst actually joins the downstream queue. While a flow burst is in transit between nodes 1 and 2, let $x_{12}(t)$ be its size, i.e., the flow content of the physical space separating node 1 from the downstream queue 2. For simplicity, we assume that each flow burst is maintained during this process (i.e., the burst may not be separated in two or more sub-bursts). We will use L to denote the physical distance between nodes.

Predicting the time when the first flow burst actually joins queue 2 is complicated by the fact that $x_2(t)$ evolves according to (1) while this burst is in transit. This is made clearer through the example in Fig. 2 which we will use to describe the evaluation of this time through a sequence of events denoted by $\{J_0, J_1, \dots, J_K\}$. We define J_0 to be the event when the flow burst leaves node 1, i.e., the occurrence of a switch from $u_1(t^-) = 0$ to $u_1(t) = 1$, and let σ_0 be its associated occurrence time. Therefore, an estimate of the

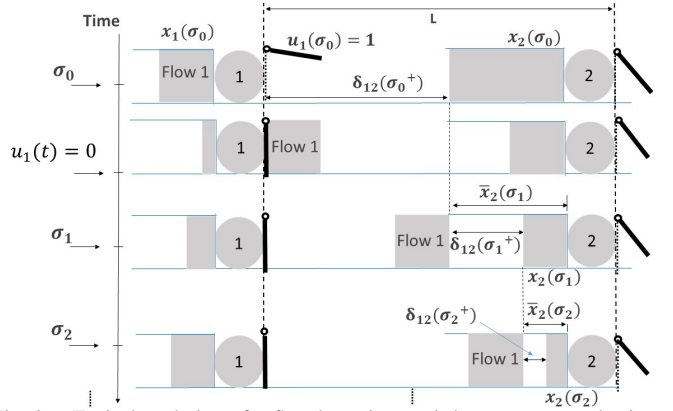


Fig. 2. Typical evolution of a flow burst in transit between two nodes in a SFM.

time when the flow burst joins the tail of queue 2, denoted by σ_1 , is given by

$$\sigma_1 = \sigma_0 + \frac{L - x_2(\sigma_0)}{v(\sigma_0)}$$

where $v(\sigma_0)$ is the speed of the flow burst. For notational simplicity, we assume this to be constant and set to $v(t) = 1$ (it will become clear in the sequel that this can be relaxed in the context of IPA). Let J_1 be the event at time σ_1 when the flow burst covers the distance $L - x_2(\sigma_0)$. In general, however, $x_2(\sigma_1) \leq \bar{x}_2(\sigma_1) = x_2(\sigma_0)$, as illustrated in the example of Fig. 2, since it is possible that $\dot{x}_2(t) = -\beta_2(t)$ for some $t \in (\sigma_0, \sigma_1)$. Thus, at $t = \sigma_1$ we may repeat the same process of estimating the time of the next opportunity that the flow burst might join queue 2 at time σ_2 to cover the distance $\bar{x}_2(\sigma_1) - x_2(\sigma_1)$ and define this potential *joining event* as J_2 , as shown in Fig. 2. Event J_K occurring at time σ_K is the last event in the sequence $\{J_0, J_1, \dots, J_K\}$ when $\bar{x}_2(\sigma_K) = x_2(\sigma_K)$. Note that this may occur either when (i) $\bar{x}_2(\sigma_K) = x_2(\sigma_K) > 0$, in which case the estimate $\bar{x}_2(\sigma_K)$ incurs no error because $x_2(\sigma_K) = x_2(\sigma_{K-1})$, i.e., the queue length at node 2 remained unchanged because $\beta_2(t) = 0$ for $t \in [\sigma_{K-1}, \sigma_K]$, or (ii) $\bar{x}_2(\sigma_K) = x_2(\sigma_K) = 0$, in which case the flow burst joins node 2 while this queue is empty. It is also clear from this process that, in the worst case, the flow burst travels the finite distance L to find $x_2(\sigma_K) = 0$.

We now formalize this process by defining a state variable $\delta_{12}(t)$ with the following dynamics (including a reset condition):

$$\dot{\delta}_{12}(t) = 0 \quad (2)$$

$$\delta_{12}(t^+) = \begin{cases} L - x_2(t) & \text{if } J_0 \text{ occurs} \\ \bar{x}_2(t) - x_2(t) & \text{if } J_k \text{ occurs, } k > 0 \end{cases}$$

where the dynamics of $\bar{x}_2(t)$ are

$$\dot{\bar{x}}_2(t) = 0 \quad (3)$$

$$\bar{x}_2(t^+) = x_2(t) \text{ if } J_k \text{ occurs, } k \geq 0$$

In addition, the following reset condition must be added to (1) for $i = 2$:

$$x_2(\sigma_K^+) = x_2(\sigma_K) + x_{12}(\sigma_K) \quad (4)$$

where the dynamics of $x_{12}(t)$ are given by

$$\dot{x}_{12}(t) = \begin{cases} 0 & \text{if } u_1(t) = 0 \\ \alpha_1(t) & \text{if } x_1(t) = 0, \alpha_1(t) \leq \beta_1(t) \\ h_1(t) & \text{otherwise} \end{cases} \quad (5)$$

$$x_{12}(t^+) = 0 \text{ if } J_K \text{ occurs}$$

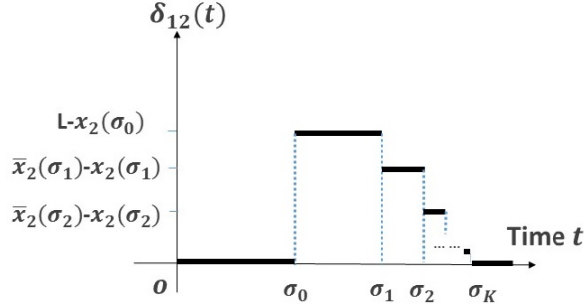


Fig. 3. Typical trajectory of $\delta_{12}(t)$ over time.

The interpretation of $\delta_{12}(t)$ is the distance between the head of a flow burst and the tail of queue 2 at time t . This is updated only at the times when events J_0, J_1, \dots, J_K take place. The evolution of $\delta_{12}(t)$ is illustrated in Fig. 3. It takes the value $\delta_{12}(t^+) = L - x_2(t)$ whenever an event J_0 occurs, i.e., a new flow burst is generated at node 1, and is piecewise constant, monotonically nonincreasing until $\delta_{12}(t^+) = 0$ when event J_K occurs, i.e., the flow burst joins queue 2. Note that in this modeling framework, we assume that $x_2(t)$ is observable at event times $\sigma_0, \sigma_1, \dots, \sigma_K$ when events J_0, J_1, \dots, J_K take place. As a final step, we generalize this model to include multiple flow bursts that may be generated in an interval $(t_1, t_2]$ such that $u_1(t) = 1$ for $t \in [t_1, t_2]$, $u_1(t_1^-) = 0$. Thus, we denote by J_k^n the k th event for the n th flow burst to (potentially) join queue 2 and extend $\delta_{12}(t)$ to $\delta_{12}^n(t)$, $n = 1, 2, \dots$. We then have:

$$\dot{\delta}_{12}^n(t) = 0 \quad (6)$$

$$\delta_{12}^n(t^+) = \begin{cases} L - x_2(t) & \text{if } J_0^n \text{ occurs} \\ \bar{x}_2^n(t) - x_2(t) & \text{if } J_k^n \text{ occurs, } k > 0 \\ \delta_{12}^n(t) - x_{12}^m(t) & \text{if } J_K^n \text{ occurs, } m = 1, \dots, n-1 \end{cases}$$

$$\dot{\bar{x}}_2^n(t) = 0 \quad (7)$$

$$\bar{x}_2^n(t^+) = \begin{cases} x_2(t) & \text{if } J_k^n \text{ occurs, } k \geq 0 \\ x_2(t) + x_{12}^m(t) & \text{if } J_K^n \text{ occurs, } m = 1, \dots, n-1 \end{cases}$$

[ptb] with the obvious generalizations of (4) and (5).

III. MULTI-INTERSECTION TRAFFIC LIGHT CONTROL WITH DELAYS

In this section, we formulate the TLC problem with two intersections, as shown in Fig. 4, by including delays. Thus, we extend the SFM presented in earlier work [7] to incorporate the delay considerations presented in Section II. As before, let $\{\alpha_i(t)\}$ and $\{\beta_i(t)\}$, $i = 1, \dots, 4$, be the incoming and outgoing flow processes respectively at all four roads, where we now interpret $\alpha_i(t)$ as the random instantaneous vehicle arrival rate at time t . We define the controllable parameters θ_i to be the durations of the GREEN light for road $i = 1, \dots, 4$. Thus, the state vector is $x(\theta, t) = [x_1(\theta, t), x_2(\theta, t), x_3(\theta, t), x_4(\theta, t), x_{12}(\theta, t)]$ where $x_i(\theta, t)$ is the content of queue i and $x_{12}(\theta, t)$ is the content of the road between intersections $I1$ and $I2$.

To maintain notational simplicity, we will assume in our analysis that **(A1)** There is no more than one traffic burst in queue 12 at any one time, **(A2)** The speed of a traffic burst between intersections is constant, and **(A3)** There is no traffic coupling between $I1$ and $I2$. Assumptions **A1**, **A2** are easily relaxed (done in our simulation examples). **A3** is

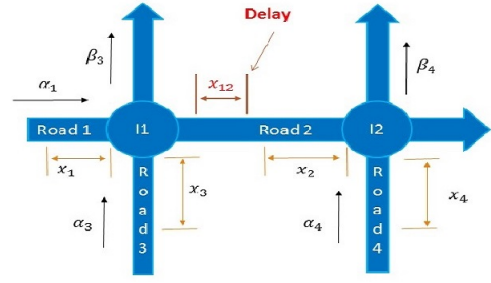


Fig. 4. Two traffic intersections.

also made to simplify the TLC problem model of and can be relaxed along the lines of [7].

We will use the notation \bar{i} to denote the index of a road perpendicular to i (e.g., $\bar{1} = 3$, $\bar{2} = 4$). We define clock state variables $z_i(t)$, $i = 1, \dots, 4$, which are associated with the GREEN light cycle for queue i as follows:

$$z_i(t) = \begin{cases} 1 & \text{if } 0 < z_i(t) < \theta_i \text{ or } z_i(t) = \theta_i \\ 0 & \text{otherwise} \end{cases} \quad (8)$$

$$z_i(t^+) = 0 \quad \text{if } z_i(t) = \theta_i$$

For simplicity, we express the state of the i th traffic light as follows:

$$G_i(t) = \begin{cases} 1 & \text{if } 0 < z_i(t) \leq \theta_i \\ 0 & \text{otherwise} \end{cases}$$

so that $G_i(t) = 0$ means that the traffic light in road i is RED, otherwise, it is GREEN. Accordingly, the departure rate $\beta_i(t)$, $i = 1, \dots, 4$ is

$$\beta_i(t) = \begin{cases} \alpha_i(t) & \text{if } G_i(t) = 1, x_i(t) = 0 \\ 0 & \text{if } G_i(t) = 0 \\ h_i(t) & \text{otherwise} \end{cases}$$

where $h_i(t)$ is the instantaneous vehicle departure rate when the traffic light of road i is GREEN and road i is not empty. The queue content dynamics for $i = 1, 3, 4$ are given by

$$\dot{x}_i(t) = \begin{cases} \alpha_i(t) & \text{if } G_i(t) = 0 \\ 0 & \text{if } x_i(t) = 0, \alpha_i(t) \leq \beta_i(t) \\ \alpha_i(t) - h_i(t) & \text{otherwise} \end{cases} \quad (9)$$

In order to provide the dynamics of $x_2(t)$ and $x_{12}(t)$, we will make use of our analysis in Section II. In particular, let σ_0 be the time when a positive traffic flow is generated from queue 1 and enters queue 12, i.e., the light turns from RED to GREEN for road 1 and $x_1(\sigma_0) > 0$. We will refer to this as event S_{12} . Invoking (2), we define $\delta_{12}(t)$ to be the distance between the head of the “transit queue” 12 and the tail of queue 2. Thus, $\delta_{12}(\sigma_0^+) = L - x_2(\sigma_0)$. We also associate a clock to this queue, denoted by $z_{12}(t)$ and initialized at $z_{12}(\sigma_0) = 0$; its purpose is to time the event which occurs when the flow burst initiated at $t = \sigma_0$ covers the distance $\delta_{12}(\sigma_0^+) = L - x_2(\sigma_0)$, i.e., $z_{12}(t) = \delta_{12}(t)/v_1$ where v_1 is the speed of vehicles leaving road 1. We define the event that occurs at this time as J_{12} . This leads to the clock dynamics

$$\dot{z}_{12}(t) = \begin{cases} 1 & \text{if } \delta_{12}(t) > 0 \\ 0 & \text{otherwise} \end{cases} \quad (10)$$

$$z_{12}(t^+) = 0 \quad \text{if } z_{12}(t) = \delta_{12}(t)/v_1$$

Recall that a J_{12} event represents a *potential* joining of the flow burst from $I1$ with queue 2. The *actual* joining event

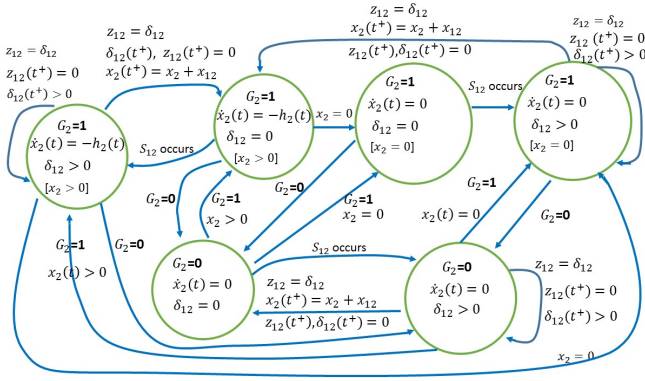


Fig. 5. Stochastic Hybrid Automaton model for $x_2(t)$.

occurs when $\delta_{12}(t^+) = 0$ from its initial value $\delta_{12}(\sigma_0^+) = L - x_2(\sigma_0)$ (see Fig. 3). Adapting (2) and (3) to the TLC setting we get

$$\begin{aligned} \dot{\delta}_{12}(t) &= 0 \\ \delta_{12}(t^+) &= \begin{cases} L - x_2(t) & \text{if } z_3(t) = \theta_3, x_1(t) + \alpha_1(t) > 0 \\ & \text{or } G_1(t) = 1, x_1(t) = 0, \\ & \alpha_1(t) \leq 0, \alpha_1(t^+) > 0 \\ \bar{x}_2(t) - x_2(t) & \text{if } z_{12}(t) = \delta_{12}(t)/v_1, \delta_{12}(t) > 0 \end{cases} \end{aligned} \quad (11)$$

$$\begin{aligned} \dot{x}_2(t) &= 0 \\ \bar{x}_2(t^+) &= x_2(t) \quad \text{if } z_3(t) = \theta_3, x_1(t) + \alpha_1(t) > 0 \\ &\quad \text{or } G_1(t) = 1, x_1(t) = 0, \alpha_1(t) \leq 0, \\ &\quad \alpha_1(t^+) > 0 \\ &\quad \text{or } z_{12}(t) = \delta_{12}(t)/v_1, \delta_{12}(t) > 0 \end{aligned} \quad (12)$$

The first case in the reset conditions above corresponds to the light turning GREEN for road 1 (RED for road 3) with a nonempty queue, the second captures the possibility of queue 1 becoming nonempty while the light is GREEN, and the third corresponds to a J_{12} event which is still not an actual joining of the flow burst with queue 2.

We can now also express the dynamics of $x_2(t)$ and $x_{12}(t)$ as follows:

$$\dot{x}_2(t) = \begin{cases} -h_2(t) & \text{if } G_2(t) = 1, x_2(t) > 0 \\ 0 & \text{otherwise} \end{cases} \quad (13)$$

$$x_2(t^+) = x_2(t) + x_{12}(t) \quad \text{if } z_{12}(t) = \delta_{12}(t)/v_1, \delta_{12}(t^+) = 0$$

$$\dot{x}_{12}(t) = \begin{cases} 0 & \text{if } G_1(t) = 0 \\ \alpha_1(t) & \text{if } x_1(t) = 0, \alpha_1(t) \leq \beta_1(t) \\ h_1(t) & \text{otherwise} \end{cases} \quad (14)$$

$$x_{12}(t^+) = 0 \quad \text{if } z_{12}(t) = \delta_{12}(t)/v_1, \delta_{12}(t^+) = 0$$

A. SFM Events

The hybrid system with dynamics given by (8)-(14) defines the SFM for the TLC problem. We now define the complete event set associated with all discontinuous state transitions in (8)-(14). The sample path of any queue content process in our model can be partitioned into *Non-Empty Periods* (NEPs) when $x_i(t) > 0$, $x_{12}(t) > 0$ and *Empty Periods* (EPs) when $x_i = 0$, $x_{12}(t) = 0$. Let us define the start of a NEP at queue i as event S_i (S_{12} for queue 12) and the end of a NEP at queue i as event E_i (E_{12} for queue 12). In view of (8)-(14), there are five events that can affect any of the processes $\{x_i(t)\}$, $i = 1, \dots, 4$, and $\{x_{12}(t)\}$:

1. E_i : $x_i(t)$ switches from a strictly positive value to zero, thus ending a NEP at queue i .
2. Γ_i : $\alpha_i(t) - \beta_i(t)$ switches from a non-positive to a strictly positive value. This may trigger an S_i event, e.g., see (9).
3. J_{12} : $z_{12}(t) = \delta_{12}(t)/v_1$ representing a potential joining of the flow burst $x_{12}(t)$ with $x_2(t)$ if $\delta_{12}(t^+) > 0$ and the actual joining when $\delta_{12}(t^+) = 0$.
4. $G2R_i$: traffic light in road i changes from GREEN to RED.
5. $R2G_i$: traffic light in road i changes from RED to GREEN.

Let us now identify the event set that affects the dynamics of queue content process:

$$\Phi_i = \{S_i, E_i, G2R_i, R2G_i\}, \quad i = 1, 3, 4$$

$$\Phi_2 = \{S_2, E_2, R2G_2, G2R_2, J_{12}\}$$

$$\Phi_{12} = \{S_{12}, E_{12}, E_1, G2R_1, J_{12}\}$$

In Φ_i , event S_i is induced by either Γ or $R2G_i$. In Φ_2 , event J_{12} is included since it affects $x_2(t)$ through the reset condition in (13). Moreover, S_2 may now also be induced by some J_{12} (if it occurs when $x_2(t) = 0$). In Φ_{12} , event S_{12} is induced by either Γ or $R2G_1$ and E_{12} is induced by J_{12} .

Figure 5 shows the hybrid automaton model for queue 2 in terms of its six possible modes depending on the values of $x_2(t)$, $G_2(t)$, and $\delta_{12}(t)$. Similar models can be drawn for the remaining queuing processes, all of which are generally interdependent (e.g., in Fig. 5 some reset conditions involve $x_{12}(t)$).

B. Cost Functions

The objective of the TLC problem is to control parameters θ_i , $i = 1, \dots, 4$, so as to minimize traffic congestion in the region covered by the two intersections in Fig. 4. In [14] and [10], the average total weighted queue lengths over a fixed time interval $[0, T]$ is used to capture congestion:

$$L(\theta; x(0), z(0), T) = \frac{1}{T} \sum_{i=1}^5 \int_0^T w_i x_i(\theta, t) dt. \quad (15)$$

where w_i is the weight associated with queue i . For convenience, we will refer to (15) as the *average queue cost function*; with a slight abuse of notation we have re-indexed $x_{12}(t)$ as $x_5(t)$. However, this may not be an adequate measure of “congestion”. For instance, it is possible that the average queue lengths over $[0, T]$ are relatively small, while reaching large values over small intervals (peak periods during a typical day). Thus, instead of restricting ourselves to (15), we define next two new cost functions.

1. Average weighted N th power of the queue lengths over a fixed interval $[0, T]$, where $N > 1$. The sample function is

$$L(\theta; x(0), z(0), T) = \frac{1}{T} \sum_{i=1}^5 \int_0^T w_i x_i^N(\theta, t) dt.$$

Observing that $x_i(\theta, t) = 0$ during an EP of queue i , we can rewrite this as

$$L(\theta; x(0), z(0), T) = \frac{1}{T} \sum_{i=1}^5 \sum_{m=1}^{M_i} \int_{\xi_{i,m}}^{\eta_{i,m}} w_i x_i^N(\theta, t) dt, \quad (16)$$

in which M_i is the total number of NEPs of queue i over a time interval $[0, T]$ and $\xi_{i,m}$, $\eta_{i,m}$ are the occurrence times of the m th S_i event and E_i event respectively. We also define

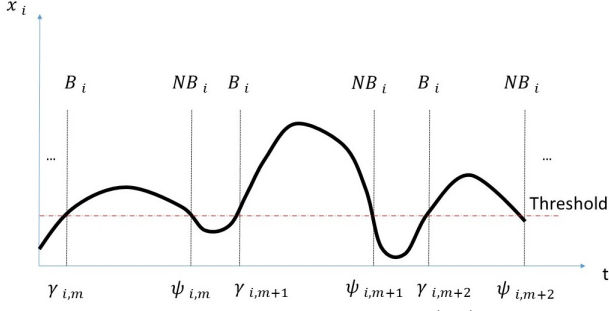


Fig. 6. Typical sample path of $y_i(\theta, t)$.

the cost incurred within the m th NEP of queue i as

$$L_{i,m}(\theta) = \int_{\gamma_{i,m}}^{\psi_{i,m}} w_i x_i^N(\theta, t) dt. \quad (17)$$

Clearly, when $N = 1$, (16) is reduced to (15). When $N > 1$, (16) amplifies the presence of intervals where queue lengths are large. Therefore, minimizing (16) decreases the probability that a road develops a large queue length. We will refer to this metric (16) as the *power cost function*.

2. Average weighted fraction of time that queue lengths exceed given thresholds over a fixed interval $[0, T]$. The sample function is

$$\begin{aligned} L(\theta; x(0), z(0), T) &= \frac{1}{T} \sum_{i=1}^5 \int_0^T w_i \mathbf{1}[x_i(\theta, t) > \zeta_i] dt \\ &= \frac{1}{T} \sum_{i=1}^5 \int_0^T w_i y_i(\theta, t) dt \end{aligned} \quad (18)$$

where ζ_i is a given threshold and $y_i(\theta, t) = \mathbf{1}[x_i(\theta, t) > \zeta_i]$. This necessitates the definition of two additional events: Z_i is the event such that $x_i(\theta, t) = \zeta_i$, $x_i(\theta, t^-) < \zeta_i$ (i.e., the queue content reaches the threshold from below) and \bar{Z}_i is the event such that $x_i(\theta, t) < \zeta_i$, $x_i(\theta, t^-) = \zeta_i$. Observe that $\dot{y}_i(\theta, t) = 0$ with a reset condition $y_i(\theta, t^+) = 1$ if $x_i(\theta, t^-) < \zeta_i$, $x_i(\theta, t^+) = \zeta_i$ and $y_i(\theta, t^+) = 0$ if $x_i(\theta, t^-) = \zeta_i$, $x_i(\theta, t^+) < \zeta_i$. Finally, we use $L_{i,m}(\theta)$ as in (17), for the cost associated with the m th NEP at queue i :

$$L_{i,m}(\theta) = \int_{\gamma_{i,m}(\theta)}^{\psi_{i,m}(\theta)} w_i y_i(\theta, t) dt. \quad (19)$$

where $\gamma_{i,m}$, $\psi_{i,m}$ are the start and end respectively of an interval such that $y_i(\theta, t) = 1$.

C. Optimization

Our purpose is to minimize the cost functions defined in (15), (16) and (18). We define the overall cost function as follows:

$$J(\theta; x(0), z(0), T) = E[L(\theta; x(0), z(0), T)],$$

in which $L(\theta; x(0), z(0), T)$ is a sample cost function of the form (15), (16) or (18). Clearly, we cannot derive a closed-form expression for the expectation above. However, we can estimate the gradient $\nabla J(\theta)$ through the sample gradient $\nabla L(\theta)$ based on IPA, which has been shown to be unbiased under mild technical conditions (Proposition 1 in [2]). Specifically, under the assumption that $\alpha_i(t)$ and $h_i(t)$ are piecewise continuous w.p.1., it holds that $dL/d\theta_j$ exists w.p.1 for all $\theta_i \in \mathbb{R}^+$, and $L(\theta)$ is Lipschitz continuous with a Lipschitz constant which has a finite first moment. We

emphasize that no explicit knowledge of $\alpha_i(t)$ and $h_i(t)$ is necessary to estimate $\nabla J(\theta)$. The IPA estimators derived in the next section only need estimates of $\alpha_i(\tau_k)$ and $h_i(\tau_k)$ at certain event times τ_k . Using $\nabla L(\theta)$, we can use a simple gradient-descent optimization algorithm to minimize the associated cost metric through the iterative scheme

$$\theta_{j,k+1} = \theta_{j,k} - c_k Q_{j,k}(\theta_k, x(0), T, \omega_k),$$

in which $Q_{j,k}(\theta_k, x(0), T, \omega_k)$ is an estimator of $dJ/d\theta_j$ (in our case, $dL/d\theta_j$) in sample path ω_k and c_k is the step size at the k th iteration [10]. In next section, we provide the IPA methodology for obtaining $dL/d\theta_j$ through the state derivatives $\frac{\partial x_i(\theta, t)}{\partial \theta_j}$.

IV. INFINITESIMAL PERTURBATION ANALYSIS (IPA)

We briefly review the IPA framework for general stochastic hybrid systems as presented in [2]. Let $\{\tau_k(\theta)\}$, $k = 1, \dots, K$, denote the occurrence times of all events in the state trajectory of a hybrid system with dynamics $\dot{x} = f_k(x, \theta, t)$ over an interval $[\tau_k(\theta), \tau_{k+1}(\theta)]$, where $\theta \in \Theta$ is some parameter vector and Θ is a given compact, convex set. For convenience, we set $\tau_0 = 0$ and $\tau_{K+1} = T$. We use the Jacobian matrix notation: $x'(t) \equiv \frac{\partial x(\theta, t)}{\partial \theta}$ and $\tau'_k \equiv \frac{\partial \tau_k(\theta)}{\partial \theta}$, for all state and event time derivatives. It is shown in [2] that

$$\frac{d}{dt} x'(t) = \frac{\partial f_k(t)}{\partial x} x'(t) + \frac{\partial f_k(t)}{\partial \theta}, \quad (20)$$

for $t \in [\tau_k, \tau_{k+1})$ with boundary condition:

$$x'(\tau_k^+) = x'(\tau_k^-) + [f_{k-1}(\tau_k^-) - f_k(\tau_k^+)] \tau'_k \quad (21)$$

for $k = 1, \dots, K$. In order to complete the evaluation of $x'(\tau_k^+)$ in (21), we need to determine τ'_k . If the event at τ_k is *exogenous* (i.e., independent of θ), $\tau'_k = 0$. However, if the event is *endogenous*, there exists a continuously differentiable function $g_k : \mathbb{R}^n \times \Theta \rightarrow \mathbb{R}$ such that $\tau_k = \min\{t > \tau_{k-1} : g_k(x(\theta, t), \theta) = 0\}$ and

$$\tau'_k = - \left[\frac{\partial g_k}{\partial x} f_k(\tau_k^-) \right]^{-1} \left[\frac{\partial g_k}{\partial \theta} + \frac{\partial g_k}{\partial x} x'(\tau_k^-) \right] \quad (22)$$

as long as $\frac{\partial g_k}{\partial x} f_k(\tau_k^-) \neq 0$.

In our TLC setting, we will use the notation

$$x'_{i,j}(t) = \frac{\partial x_i(\theta, t)}{\partial \theta_j}, z'_{i,j}(t) = \frac{\partial z_i(\theta, t)}{\partial \theta_j}, \tau'_{k,j}(t) = \frac{\partial \tau_k(\theta)}{\partial \theta_j}$$

We also note that in (9), (13), (14), $\frac{\partial f_k(t)}{\partial \theta} = \frac{\partial f_k(t)}{\partial x} = 0$ and (20) reduces to

$$x'_{i,j}(t) = x'_{i,j}(\tau_k^+), \quad t \in (\tau_k, \tau_{k+1}] \quad (23)$$

A. State and Event Time Derivatives

We will now apply the IPA equations (21)-(23) to our TLC setting on an event basis for each of the sets Φ_i , $i = 1, \dots, 4$, and Φ_{12} . In all cases, τ_k denotes the associated event time.

1) *IPA for Event Set* $\Phi_i = \{S_i, E_i, R2G_i, G2R_i\} \cup \{Z_i, \bar{Z}_i\}$, $i = 1, 3, 4$: IPA for these three processes for each of the events in the first set above is identical to that in [14]. Thus, we simply summarize the results here.

(1) *Event* E_i : $x'_{i,j}(\tau_k^+) = 0$.

(2) *Event* $G2R_i$: Let ρ_k be the time of the last $R2G_i$ event before $G2R_i$ occurs. Then, $\tau'_{k,j} = \mathbf{1}[j = i] + \rho'_{k,j}$ and

$$x'_{i,j}(\tau_k^+) = \begin{cases} x'_{i,j}(\tau_k) - \alpha_i(\tau_k)\tau'_{k,j} & \text{if } x_i(t) = 0, \alpha_i(t) \leq \beta_i(t) \\ x'_{i,j}(\tau_k) - h_i(\tau_k)\tau'_{k,j} & \text{otherwise} \end{cases} \quad (24)$$

(3) *Event* $R2G_i$: Let ρ_k be the time of this event and τ_k be the time of the last $G2R_i$ event before $R2G_i$ occurs. Then, $\rho'_{k,j} = \mathbf{1}[j = i] + \tau'_{k,j}$ and

$$x'_{i,j}(\rho_k^+) = \begin{cases} x'_{i,j}(\rho_k) + \alpha_i(\rho_k)\rho'_{k,j} & \text{if } x_i(t) = 0, \alpha_i(t) \leq \beta_i(t) \\ x'_{i,j}(\rho_k) + h_i(\rho_k)\rho'_{k,j} & \text{otherwise} \end{cases} \quad (25)$$

(4) *Event* S_i : If S_i is induced by $G2R_i$, then $x'_{i,j}(\tau_k^+) = x'_{i,j}(\tau_k) - \alpha_i(\tau_k)\tau'_{k,j}$. If S_i is an exogenous event triggered by Γ_i , then $x'_{12,j}(\tau_k^+) = x'_{12,j}(\tau_k)$.

For the two new events $\{Z_i, \bar{Z}_i\}$, we have:

(5) *Event* Z_i : This is an endogenous event which occurs when $g_k(x(\theta, t), \theta) = x_i(\tau_k) - \zeta_i = 0$. Applying (22), we have

$$\tau'_{k,j} = \begin{cases} -x'_{i,j}(\tau_k)/\alpha_i(\tau_k) & \text{if } G_i(t) = 0 \\ -x'_{i,j}(\tau_k)/[\alpha_i(\tau_k) - h_i(\tau_k)] & \text{if } G_i(t) = 1 \end{cases} \quad (26)$$

Moreover, based on the definition $y_i(t) = \mathbf{1}[x_i(t) > \zeta_i]$ in Section III-B, $y_i(\tau_k^+) = 1$, which implies that $y_{i,j}(\tau_k^+) + y(\tau_k^+)\tau'_{k,j} = 0$. Since $\dot{y}_i(\tau_k^+) = 0$, we get $y'_{i,j}(\tau_k^+) = 0$.

(6) *Event* \bar{Z}_i : Similar to the previous case, $g_k(x(\theta, t), \theta) = x_i(\tau_k) - \zeta_i = 0$ and applying (22) gives

$$\tau'_{k,j} = -x'_{i,j}(\tau_k)/(\alpha_i(\tau_k) - h_i(\tau_k)) \quad (27)$$

In this case, $y_i(\tau_k^+) \equiv 0$, therefore, $y'_{i,j}(\tau_k^+) + y_i(\tau_k^+)\tau'_{k,j} = 0$ and, since $\dot{y}_i(\tau_k^+) = 0$, we get $y'_{i,j}(\tau_k^+) = 0$.

2) *IPA for Event Set* $\Phi_2 = \{S_2, E_2, R2G_2, G2R_2, J_{12}\} \cup \{Z_2, \bar{Z}_2\}$: IPA for this set and for Φ_{12} is different as detailed next.

(1) *Event* E_2 : This is an endogenous event ending an EP that occurs when $g_k(x(\theta, t), \theta) = x_2(t) = 0$ at $t = \tau_k$. Applying (22) and using (13), we have $\tau'_{k,j} = x'_{2,j}(\tau_k^-)/h_2(\tau_k^-)$. It then follows from (21) that $x'_{2,j}(\tau_k^+) = x'_{2,j}(\tau_k^-) - h_2(\tau_k^-)\tau'_{k,j} = 0$.

(2) *Event* S_2 : In view of the reset condition in (13), this event is induced by J_{12} provided $\delta_{12}(t^+) = 0$. As described in Section II, a sequence of J_{12} events is initiated when a flow burst is generated at node 1 with associated event times $\{\sigma_0, \sigma_1, \dots, \sigma_K\}$. Event S_2 is induced by the last occurrence of a J_{12} event at time σ_K . Thus, our goal here is to evaluate the IPA derivative $x'_{2,j}(\sigma_K^+)$. At first sight, it would appear that this requires the complete sequence $\{x'_{2,j}(\sigma_0^+), \dots, x'_{2,j}(\sigma_{K-1}^+)\}$ along with event time derivatives $\{\sigma'_{0,j}, \dots, \sigma'_{K-1,j}\}$ from which $x'_{2,j}(\sigma_K^+)$ can be inferred. However, the following lemma helps us show that the only information needed from the full sequence of J_{12} events is σ'_0 .

Lemma 1. Let σ_k , $k = 0, 1, \dots, K$ be the occurrence time of the k th J_{12} event for a flow burst initiated at σ_0 . Then,

$$\sigma'_{k,j} = \frac{-1}{v_1} [x'_{2,j}(\sigma_{k-1}) + \dot{x}_2(\sigma_{k-1})\sigma'_{k-1,j}] + \sigma'_{0,j}$$

Proof: Event J_{12} at $t = \sigma_k$ is endogenous and occurs when $g_k(x(\theta, \sigma_k), \theta) = z_{12}(\sigma_k) - \delta_{12}(\sigma_k)/v_1 = 0$. Applying (22) and using (10),(11), we get $\sigma'_{k,j} = \delta'_{12,j}(\sigma_k)/v_1 - z'_{12,j}(\sigma_k)$. Using (23), we have $\delta'_{12,j}(\sigma_k) = \delta'_{12,j}(\sigma_{k-1}^+)$ and it follows that

$$\sigma'_{k,j} = \delta'_{12,j}(\sigma_{k-1}^+)/v_1 - z'_{12,j}(\sigma_k) \quad (28)$$

Again applying (23) gives $z'_{12,j}(\sigma_k) = z'_{12,j}(\sigma_{k-1}^+)$. From (21), in view of (10), we get, for $k = 1$, $z'_{12,j}(\sigma_0^+) = -\sigma'_{0,j}$. The reset condition in (11) implies that $\delta_{12}(\sigma_0^+) = L - x_2(\sigma_0)$, hence $\delta'_{12,j}(\sigma_0^+) = -x'_{2,j}(\sigma_0) - \dot{x}_2(\sigma_0)\sigma'_{0,j}$. Thus, in this case, (28) gives:

$$\sigma'_{1,j} = \frac{-1}{v_1} [x'_{2,j}(\sigma_0) + \dot{x}_2(\sigma_0)\sigma'_{0,j}] + \sigma'_{0,j} \quad (29)$$

For $k > 1$, based on the reset condition in (10), we have $z_{12}(\sigma_k^+) = 0$. Taking the total derivative, we get $z'_{12,j}(\sigma_k^+) = -\sigma'_{k,j}$. The reset condition in (11) now implies that $\delta_{12}(\sigma_{k-1}^+) = \bar{x}_2(\sigma_{k-1}) - x_2(\sigma_{k-1})$, hence

$$\delta'_{12,j}(\sigma_{k-1}^+) = \bar{x}'_{2,j}(\sigma_{k-1}) + \dot{\bar{x}}_2(\sigma_{k-1})\sigma'_{k-1,j} - x'_{2,j}(\sigma_{k-1}) - \dot{x}_2(\sigma_{k-1})\sigma'_{k-1,j} \quad (30)$$

Applying (23), we have $\bar{x}'_{2,j}(\sigma_{k-1}) = \bar{x}'_{2,j}(\sigma_{k-2}^+)$. Looking at (12), we have $\dot{\bar{x}}_2(\sigma_{k-1}) = 0$ and the reset condition implies that $\bar{x}'_{2,j}(\sigma_{k-2}^+) = x'_{2,j}(\sigma_{k-2}) + \dot{x}_2(\sigma_{k-2})\sigma'_{k-2,j}$. Thus, returning to (30), we get

$$\delta'_{12,j}(\sigma_{k-1}^+) = x'_{2,j}(\sigma_{k-2}) + \dot{x}_2(\sigma_{k-2})\sigma'_{k-2,j} - x'_{2,j}(\sigma_{k-1}) - \dot{x}_2(\sigma_{k-1})\sigma'_{k-1,j} \quad (31)$$

Recalling that $z'_{12,j}(\sigma_k^+) = -\sigma'_{k,j}$ and combining (29),(31) into (28), we get

$$\begin{aligned} \sigma'_{k,j} &= \sigma'_{k-1,j} + \frac{1}{v_1} [x'_{2,j}(\sigma_{k-2}) + \dot{x}_2(\sigma_{k-2})\sigma'_{k-2,j} \\ &\quad - x'_{2,j}(\sigma_{k-1}) - \dot{x}_2(\sigma_{k-1})\sigma'_{k-1,j}] \\ &= \sigma'_{0,j} + \frac{1}{v_1} [-x'_{2,j}(\sigma_{k-1}) - \dot{x}_2(\sigma_{k-1})\sigma'_{k-1,j}] \end{aligned} \quad (32)$$

where the last step follows from a recursive evaluation of $\sigma'_{k-1,j}$ using (29) and (32) leading to many of the terms above canceling. This completes the proof. ■

Let us now focus on the last J_{12} event at time σ_K . It follows from the reset condition in (13) that

$$x'_{2,j}(\sigma_K^+) = \begin{cases} x'_{2,j}(\sigma_K) + x'_{12,j}(\sigma_K) & \text{if } G_2(\sigma_K) = 1 \\ +h_2(\sigma_K^+)\sigma'_{0,j} & \text{and } x_2(\sigma_K) = 0 \\ x'_{2,j}(\sigma_K) + x'_{12,j}(\sigma_K) & \text{otherwise} \end{cases} \quad (33)$$

Recall that $\delta_{12}(\sigma_K^+) = 0$ in (33). If $G_2(\sigma_K) = 1$ and $x_2(\sigma_K) = 0$, then $x_2(\sigma_{K-1}) - x_2(\sigma_K) = 0$, hence $x_2(\sigma_{K-1}) = 0$. It follows from (13) that $\dot{x}_2(\sigma_{K-1}) = 0$. Based on Case 1 above, we get $x'_{2,j}(\sigma_{K-1}) = 0$. Then, from Lemma 1, $\sigma'_{K,j} = \sigma'_{0,j}$ and (33) becomes

$$x'_{2,j}(\sigma_K^+) = \begin{cases} x'_{2,j}(\sigma_K) + x'_{12,j}(\sigma_K) & \text{if } G_2(\sigma_K) = 1 \\ +h_2(\sigma_K^+)\sigma'_{0,j} & \text{and } x_2(\sigma_K) = 0 \\ x'_{2,j}(\sigma_K) + x'_{12,j}(\sigma_K) & \text{otherwise} \end{cases} \quad (34)$$

We conclude that the state derivative $x'_{2,j}(\sigma_K^+)$ when event S_2 occurs is independent of all event time derivatives $\sigma'_{1,j}, \dots, \sigma'_{K,j}$ and involves only $\sigma'_{0,j}$, evaluated when the associated flow burst is initiated.

(3) *Event G2R2*: This is an endogenous event that occurs when $g_k(x(\theta, t), \theta) = z_2(t) - \theta_2 = 0$. Based on (22), $\tau'_{k,j} = \mathbf{1}[j=2] - z'_{2,j}(\tau_k)$. Let ρ_k be the last $R2G_2$ before $G2R_2$ occurs. Applying (23), we have $z'_{2,j}(\rho_k^+) = z'_{2,j}(\tau_k)$. and from (21) we get $z'_{2,j}(\rho_k^+) = -\rho'_{k,j}$. It follows that $\tau'_{k,j} = \mathbf{1}[j=2] + \rho'_{k,j}$. Based on (21), we have

$$x'_{2,j}(\tau_k^+) = \begin{cases} x'_{2,j}(\tau_k) - h_2(\tau_k)\tau'_{k,j} & \text{if } x_2(\tau_k) > 0 \\ x_{2,j}(\tau_k) & \text{otherwise} \end{cases} \quad (35)$$

(4) *Event R2G2*: Let ρ_k be the time of this event and τ_k be the time of the last $G2R_2$ event before $R2G_2$ occurs. Similar to (3) above, we get $\rho'_{k,j} = \mathbf{1}[j=4] + \tau'_{k,j}$ and use this value in the expression below which follows from (21):

$$x'_{2,j}(\rho_k^+) = \begin{cases} x'_{2,j}(\rho_k) + h_2(\tau_k^+)\rho'_{k,j} & \text{if } x_2(\rho_k) > 0 \\ x_{2,j}(\rho_k) & \text{otherwise} \end{cases} \quad (36)$$

(5) *Event J12*: The analysis of this event has already been done in Case (2) above, including Lemma 1.

(6) *Event Z2*: This is an endogenous event which is triggered by J_{12} : if a traffic burst from node 1 joins $x_2(t)$ at $t = \tau_k$ and $x_2(\tau_k^+) > \zeta_2$, this results in Z_2 . Since $y_2(\tau_k^+) = 1$ and $\dot{y}_2(t) = 0$, we have $y'_{2,j}(\tau_k^+) = 0$.

(7) *Event Z2*: This is an endogenous event that occurs when $g_k(x(\theta, t), \theta) = x_2(\theta, t) - \zeta_2 = 0$. Applying (22), we have $\tau_{k,j} = x_2(\tau_k)/h_2(\tau_k)$. Moreover, $y_2(\tau_k^+) \equiv 0$, therefore, $y'_{2,j}(\tau_k^+) + y_2(\tau_k^+)\tau'_{k,j} = 0$ and, since $\dot{y}_2(\tau_k^+) = 0$, we get $y'_{2,j}(\tau_k^+) = 0$.

3) *IPA for Event Set $\Phi_{12} = \{S_{12}, E_{12}, E_1, G2R_1, J_{12}\} \cup \{Z_{12}, \bar{Z}_{12}\}$* : (1) *Event S12*: This event can be either exogenous or endogenous. If $x_1(\tau_k) > 0$ or if $x_1(\tau_k) = 0$, $\alpha_1(t) > 0$, S_{12} is induced by event $R2G_1$ which is endogenous. Otherwise, S_{12} is exogenous event and occurs when $G_1(\tau_k) = 1$ and $\alpha_1(\tau_k)$ switches from zero to some positive value.

Case (1a): S_{12} is induced by $R2G_1$. Referring to our analysis of $R2G_1$ (Case (3) for Φ_1), we have already evaluated $\tau'_{k,j}$. Then, applying (21), we get

$$x'_{12,j}(\tau_k^+) = \begin{cases} x'_{12,j}(\tau_k) - \alpha_1(\tau_k^+)\tau'_{k,j} & \text{if } x_1(\tau_k) = 0 \text{ and} \\ x_{12,j}(\tau_k) - h_1(\tau_k^+)\tau'_{k,j} & 0 < \alpha_1(\tau_k) \leq \beta_1(\tau_k) \\ & \text{otherwise} \end{cases} \quad (37)$$

Case(1b) S_{12} is exogenous. In this case, $\tau'_{k,j} = 0$ and applying (21) gives $x'_{12,j}(\tau_k^+) = x'_{12,j}(\tau_k)$.

(2) *Event E12*: This event occurs when the traffic burst in queue 12 joins queue 2. This is an endogenous event that occurs when $g_k(x(\theta, \tau_k), \theta) = z_{12}(\tau_k) - \delta_{12}(\tau_k) = 0$ and $\delta_{12}(\tau_k^+) = 0$. When this happens, it follows from the reset condition in (14) that $x'_{12,j}(\tau_k^+) = 0$.

(3) *Event E1*: This is an endogenous event that occurs when $g_k(x(\theta, t), \theta) = x_1(t) = 0$. Applying (22), we get $\tau'_{k,j} = -\frac{x'_{1,j}(\tau_k)}{\alpha_1(\tau_k) - h_1(\tau_k)}$. Thus, using (21), we get

$$x'_{12,j}(\tau_k^+) = x'_{12,j}(\tau_k) + (h_1(\tau_k) - \alpha_1(\tau_k))\tau'_{k,j} = x'_{12,j}(\tau_k) + x'_{1,j}(\tau_k) \quad (38)$$

(4) *Event G2R1*: This is an endogenous event that occurs when $g_k(x(\theta, t), \theta) = z_1(t) - \theta_1 = 0$. It was shown under the analysis for events in Φ_1 that for $G2R_1$ we have $\tau'_{k,j} = \mathbf{1}[j=i] + \rho'_{k,j}$ where ρ_k is the time of the last $R2G_1$ event before $G2R_1$ occurs. Using this value, we can evaluate the following which follows from (21):

$$x'_{12,j}(\tau_k^+) = \begin{cases} x'_{12,j}(\tau_k) + \alpha_1(\tau_k)\tau'_{k,j} & \text{if } x_1(\tau_k) = 0 \\ & \text{and } \alpha_1(t) \leq \beta_1(t) \\ x'_{12,j}(\tau_k) + h_1(\tau_k)\tau'_{k,j} & \text{otherwise} \end{cases} \quad (39)$$

(5) *Event J12*: The analysis of this event has already been done in Case (2) above, including Lemma 1.

(6) *Event Z12*: This is an endogenous event that occurs when $g_k(x(\theta, t), \theta) = x_{12}(\theta, t) - \zeta_{12} = 0$. Applying (22), we have

$$\tau'_{k,j} = \begin{cases} -\frac{x'_{12,j}(\tau_k)}{\alpha_1(\tau_k)} & \text{if } x_1(\tau_k) = 0 \\ & \text{and } \alpha_1(t) \leq \beta_1(t) \\ -\frac{x'_{12,j}(\tau_k)}{h_1(\tau_k)} & \text{otherwise} \end{cases}$$

Since $y_{12}(\tau_k^+) = 1$ and $\dot{y}_{12}(t) = 0$, we have $y'_{12,j}(\tau_k^+) = 0$.

(7) *Event Z12*: This is triggered by event E_{12} when the traffic burst in queue 12 joins queue 2 and we reset $x_{12}(\tau_k^+) = 0$. Since $y_{12}(\tau_k^+) = 0$ and $\dot{y}_{12}(t) = 0$, we have $y'_{12,j}(\tau_k^+) = 0$.

B. Cost Function Derivatives

Returning to (15), (16), and (18), recall that the IPA estimator consists of the gradient formed by the sample performance derivatives $\frac{dL}{d\theta_j}$, which in turn depend on the state derivatives that we have evaluated in the previous section. The derivation of the IPA estimator for the Average Queue cost function in (15) is similar to that in [14] and related prior work and is omitted. Instead, we concentrate on the two new cost functions (16), and (18).

For the Power cost function, we derive $\frac{dL_{i,m}(\theta)}{d\theta_j}$ from (17), from which $\frac{dL}{d\theta_j}$ is obtained by adding over all M_i NEPs of each queue i over $[0, T]$:

$$\begin{aligned} \frac{dL_{i,m}(\theta)}{d\theta_j} &= N x'_{i,j}(\theta, t) \int_{\xi_{i,m}(\theta)}^{\eta_{i,m}(\theta)} w_i x_i^{N-1}(\theta, t) dt \\ &= N [x'_{i,j}(\xi_{i,m}^+) \int_{\xi_{i,m}(\theta)}^{t_{i,m}^1} w_i x_i^{N-1}(\theta, t) dt \\ &\quad + \sum_{j=2}^{J_{i,m}} x'_{i,j}((t_{i,m}^j)^+) \int_{t_{i,m}^{j-1}}^{t_{i,m}^j} w_i x_i^{N-1}(\theta, t) dt \\ &\quad + x'_{i,j}((t_{i,m}^{J_{i,m}})^+) \int_{t_{i,m}^{J_{i,m}-1}}^{\eta_{i,m}(\theta)} w_i x_i^{N-1}(\theta, t) dt], \end{aligned}$$

where $t_{i,m}^j, j = 1, \dots, J_{i,m}$ is the occurrence time of the j th event in the m th NEP of queue i . The state derivative is determined on an event-driven basis using $x'_{i,j}(\tau_k^+)$ corresponding to the event occurring at time τ_k ; for instance, if $G2R_1$ occurs at node 1, then (24) is invoked with $i = 1$.

For the Threshold cost function, we know that $y'(\theta, t) = 0$ and it follows from (19):

$$\begin{aligned} \frac{dL_{i,m}(\theta)}{d\theta_j} &= \int_{\gamma_{i,m}(\theta)}^{\psi_{i,m}(\theta)} w_i y'_{i,j}(\theta, t) dt - w_i y_i(\theta, \gamma_{i,m}^+) \gamma'_{i,m,j} \\ &\quad + w_i y_i(\theta, \psi_{i,m}^-) \psi'_{i,m,j} \\ &= w_i (\psi'_{i,m,j} - \gamma'_{i,m,j}), \end{aligned}$$

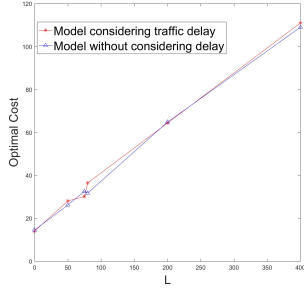


Fig. 7. Comparison of Optimal Average Queue Cost vs L.

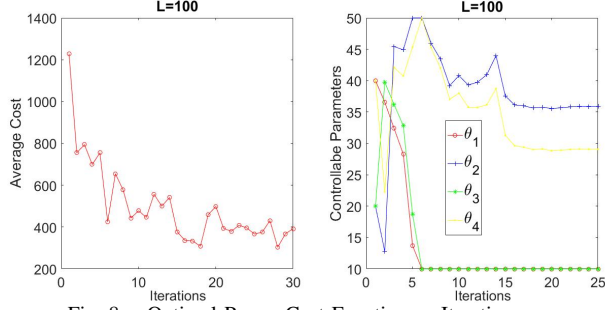


Fig. 8. Optimal Power Cost Function vs Iterations.

Note that in this case the derivative depends only on $\psi'_{i,m,j}$, $\gamma'_{i,m,j}$, the event time derivatives in (26),(27) for $i = 1, 3, 4$ and the corresponding event time derivatives in Cases (6),(7) for each of sets Φ_{22} and Φ_{12} .

V. SIMULATION RESULTS

In this section, we use the derived IPA estimators in order to optimize the green light cycles in the two-intersection model of Fig. 4. We stress that this model is simulated as a Discrete Event System (DES) with individual vehicles rather than flows, so that the resulting estimators are based on actual observed data. This is made possible by the fact that all SFM events in the sets Φ_i , $i = 1, \dots, 4$, and Φ_{12} coincide with those of the DES, therefore they are directly observable along with their occurrence times.

We assume that all vehicle arrival processes are Poisson (recall, however, that IPA is *independent of these distributions*) with rates $\bar{\alpha}_i$, $i = 1, 3, 4$, and that the vehicle departure rate $h_i(t)$ on each non-empty road is constant. Moreover, we limit each controllable parameter so that $\theta_i \in [\theta_{i,min}, \theta_{i,max}]$. In our simulations, $\alpha_i(\tau_k)$ is estimated through N_a/t_w by counting the number of arriving vehicles N_a over a time interval $[0, t_w]$ and $h_i(t)$ is estimated using the same method as in [10]. Three sets of simulations are presented below, one for each of the three cost metrics in (15), (16) and (18).

1. Average Queue Cost Function. We minimize metric (15), over $[0, T]$. All three arrival processes are Poisson with rates $\bar{\alpha} = [0.41, 0.45, 0.32]$ and the departure rates at roads 1, 2, 3, 4 are $[1.2, 1.3, 1.2, 1.1]$. We choose $T = 1000s$, $w_i = 1$ and $\theta_i \in [10, 50]$ for all i , and the initial θ_i values are $[40, 20, 20, 40]$. Figure 7 shows the optimal cost (averaged over 10 sample paths) considering the transit delay between intersections (red curve) and ignoring this delay (blue curve) as a function of L . In this case, delay has no effect on the long term total average queue length, as expected. However, as pointed out earlier, this metric does not accurately capture traffic congestion.

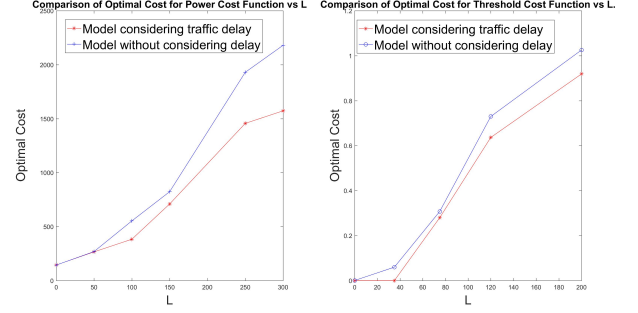


Fig. 9. Comparison of Optimal Cost with/without delay vs L.

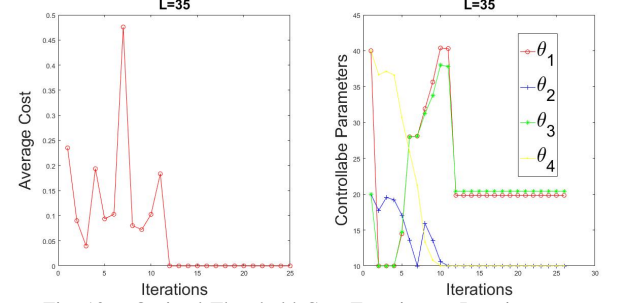


Fig. 10. Optimal Threshold Cost Function vs Iterations.

2. Power Cost Function, $N = 2$. For the same settings as before and a quadratic queuing cost, Fig. 8 shows how this cost function and the associate controllable parameters converge when $L = 100$, achieving a 40% cost decrease. In the left plot of Fig. 9, we compare the optimal cost considering the transit delay between intersections and ignoring this delay. Clearly, including delays in our IPA estimators for $L > 0$ achieves a lower cost, with the gap increasing as L increases.

3. Threshold Cost Function. For the same settings and a common threshold $\zeta_i = 25$ for all i and with $L = 35$, Fig. 10 shows how this cost function and the associate controllable parameters converge, with the cost converging to its zero lower bound, therefore, in this case we have a guarantee that our approach reaches the global optimum. In the right plot of Fig. 9, we compare the optimal cost considering the transit delay between intersections and ignoring this delay. Once again, including delays achieves a lower cost, with the gap increasing as L increases.

In Fig. 11, we provide histograms of the queue contents when $L = 35$. On the left, the controllable parameters are at their initial values $[40, 20, 20, 40]$ and we can see that queues 2, 3, and 12 frequently exceed the threshold. Under the optimal solution we obtain (right side) taking the transit delay between intersections into account, observe that no queue ever exceeds the threshold over $[0, T]$, hence the optimal cost 0 is obtained. Moreover, note that the probabilities that $x_2(t) = 0$ and $x_3(t) = 0$ significantly increase indicating a much improved traffic balance.

VI. CONCLUSIONS AND FUTURE WORK

We have presented an extended SFM to allow for delays which can arise in the flow movement. We have applied this framework to the multi-intersection traffic light control problem by including transit delays for vehicles moving from one intersection to the next. We have developed IPA for this extended SFM in order to derive on-line gradient estimates of several congestion cost metrics with respect

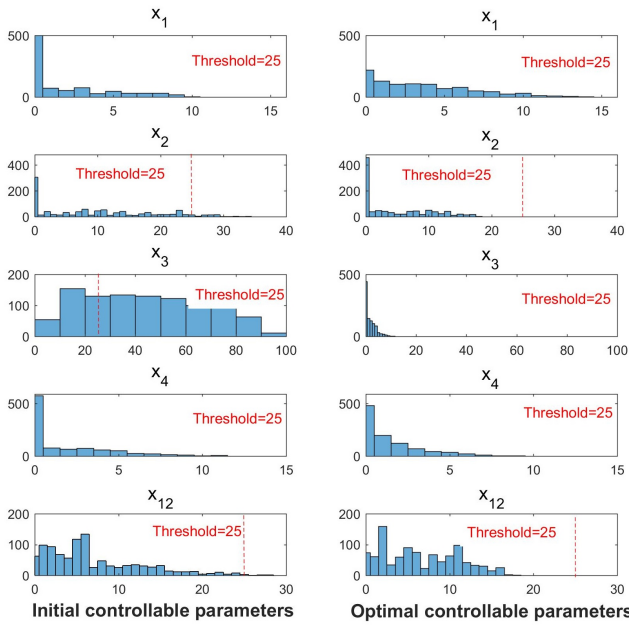


Fig. 11. Distribution of queue lengths under $L = 35$.

to the controllable green and red cycle lengths, including two new cost metrics that better capture congestion. Our simulation results show that the inclusion of delays in our analysis leads to improved performance relative to models that ignore delays. Future work aims at extensions to allow traffic blocking between intersections and allowing multiple traffic bursts between intersections.

REFERENCES

- [1] C. G. Cassandras and S. Lafortune, *Introduction to discrete event systems*. Springer Science & Business Media, 2009.
- [2] C. G. Cassandras, Y. Wardi, C. G. Panayiotou, and C. Yao, "Perturbation analysis and optimization of stochastic hybrid systems," *European Journal of Control*, vol. 6, no. 6, pp. 642–664, 2010.
- [3] M. Armony, S. Israelit, A. Mandelbaum, Y. N. Marmor, Y. Tseytlin, G. B. Yom-Tov *et al.*, "On patient flow in hospitals: A data-based queueing-science perspective," *Stochastic Systems*, vol. 5, no. 1, pp. 146–194, 2015.
- [4] S. Yin, S. X. Ding, A. H. Abandan Sari, and H. Hao, "Data-driven monitoring for stochastic systems and its application on batch process," *International Journal of Systems Science*, vol. 44, no. 7, pp. 1366–1376, 2013.
- [5] M. P. Anderson, W. W. Woessner, and R. J. Hunt, *Applied groundwater modeling: simulation of flow and advective transport*. Academic press, 2015.
- [6] C. G. Cassandras, Y. Wardi, B. Melamed, G. Sun, and C. G. Panayiotou, "Perturbation analysis for on-line control and optimization of stochastic fluid models," *IEEE Transactions on Automatic Control*, vol. 47, no. 8, pp. 1234–1248, 2002.
- [7] Y. Geng and C. G. Cassandras, "Multi-intersection traffic light control with blocking," *Discrete Event Dynamic Systems*, vol. 25, no. 1-2, pp. 7–30, 2015.
- [8] Y. Wardi, R. Adams, and B. Melamed, "A unified approach to infinitesimal perturbation analysis in stochastic flow models: the single-stage case," *IEEE Transactions on Automatic Control*, vol. 55, no. 1, pp. 89–103, 2010.
- [9] C. Yao and C. G. Cassandras, "Perturbation analysis of stochastic hybrid systems and applications to resource contention games," *Frontiers of Electrical and Electronic Engineering in China*, vol. 6, no. 3, pp. 453–467, 2011.
- [10] J. L. Fleck, C. G. Cassandras, and Y. Geng, "Adaptive quasi-dynamic traffic light control," *IEEE Transactions on Control Systems Technology*, vol. 24, no. 3, pp. 830–842, 2016.
- [11] L. Head, F. Ciarallo, and D. L. Kaduwela, "A perturbation analysis approach to traffic signal optimization," *INFORMS National Meeting*, 1996.
- [12] M. C. Fu and W. C. Howell, "Application of perturbation analysis to traffic light signal timing," *Proceedings of the IEEE Conference on Decision and Control*, pp. 4837–4840, 2003.

- [13] C. G. Panayiotou, W. C. Howell, and M. C. Fu, "Online traffic light control through gradient estimation using stochastic flow models," *Proceedings of the IFAC Triennial World Congress*, 2005.
- [14] Y. Geng and C. G. Cassandras, "Traffic light control using infinitesimal perturbation analysis," in *Decision and Control (CDC), 2012 IEEE 51st Annual Conference on*. IEEE, 2012, pp. 7001–7006.